J Vet Sci. 2022 Sep;23(5):e65
https://doi.org/10.4142/jvs.22109
pISSN 1229-845X·eISSN 1976-555X

Journal of Veterinary Science

Original Article
Medical Imaging

Check for updates

Computed tomographic assessment of retrograde urohydropropulsion in male dogs and prediction of stone composition using Hounsfield unit in dogs and cats

Aurélie Bruwier [1,*], **Benjamin Godart** [2], **Laure Gatel** [1], **Dimitri Leperlier** [2], **Anne-Sophie Bedu** [1]

[1]Imaging diagnostic department, Centre Hospitalier Vétérinaire (Chv) Pommery, 51100 Reims, France
[2]Surgery department, Centre Hospitalier Vétérinaire (Chv) Pommery, 51100 Reims, France

OPEN ACCESS

Received: Apr 17, 2022
Revised: Jun 14, 2022
Accepted: Jun 28, 2022
Published online: Jul 15, 2022

***Corresponding author:**
Aurélie Bruwier
Imaging Diagnostic Department, Centre Hospitalier Vétérinaire (CHV) Pommery, 226 bd Pommery, 51100 Reims, France.
Email: a.bruwier.vet@gmail.com
https://orcid.org/0000-0001-5834-5974

ABSTRACT

Background: Persistent uroliths after a cystotomy in dogs are a common cause of surgical failure.
Objectives: This study examined the following: the success rate of retrograde urohydropropulsion in male dogs using non-enhanced computed tomography (CT), whether the CT mean beam attenuation values in Hounsfield Units (mHU) measured *in vivo* could predict the urolithiasis composition and whether the selected reconstruction kernel may influence the measured mHU.
Methods: All dogs and cats that presented with lower urinary tract uroliths and had a non-enhanced CT preceding surgery were included. In male dogs, CT was performed after retrograde urohydropropulsion to detect the remaining urethral calculi. The percentage and location of persistent calculi were recorded. The images were reconstructed using three kernels, from smooth to ultrasharp, and the calculi mHU were measured.
Results: Sixty-five patients were included in the study. The success rate of retrograde urohydropropulsion in the 45 male dogs was 55.6% and 86.7% at the first and second attempts, respectively. The predominant components of the calculi were cystine (20), struvite (15), calcium oxalate (8), and urate (7). The convolution kernel influenced the mHU values ($p < 0.05$). The difference in mHU regarding the calculus composition was better assessed using the smoother kernel. A mHU greater than 1,000 HU was predictive of calcium oxalate calculi.
Conclusions: Non-enhanced CT is useful for controlling the success of retrograde urohydropropulsion. The mHU could allow a prediction of the calculus composition, particularly for calcium oxalate, which may help determine the therapeutic strategy.

Keywords: CT Scan; dogs; feline; urethral calculi; vesical calculi; retrograde urohydropropulsion; attenuation

INTRODUCTION

Urolithiasis is common in companion animals, and urethral calculi may be particularly challenging to detect. The calculi opacity can vary in plain radiographs depending on

ORCID iDs

Aurélie Bruwier
https://orcid.org/0000-0001-5834-5974
Benjamin Godart
https://orcid.org/0000-0001-5643-8122
Laure Gatel
https://orcid.org/0000-0003-1082-222X
Dimitri Leperlier
https://orcid.org/0000-0002-5611-2875
Anne-Sophie Bedu
https://orcid.org/0000-0002-5916-1592

Author Contributions

Conceptualization: Bruwier A, Gatel L, Leperlier D, Bedu AS; Formal analysis: Gatel L, Investigation: Bruwier A, Godart B, Gatel L, Leperlier D, Bedu AS; Methodology: Bruwier A, Gatel L, Bedu AS; Resources: Leperlier D, Bedu AS; Supervision: Gatel L, Leperlier D, Bedu AS; Validation: Bruwier A, Godart B, Gatel L, Leperlier D, Bedu AS; Visualization: Bruwier A, Gatel L; Writing - original draft: Bruwier A, Godart B; Writing - review & editing: Gatel L, Leperlier D, Bedu AS.

Conflict of Interest

The authors declare no conflicts of interest.

their mineral composition [1]. Some are radiopaque, such as calcium oxalate or struvite calculi, while others are radiolucent or faintly radiopaque, such as cystine or urate calculi, and difficult to detect on plain radiographs [2]. Approximately 13% of survey radiographs fail to detect urolithiasis among all urolith types [3]. On the plain radiographs, the risk of a false negative result is higher for detecting urate, cystine, and calcium phosphate calculi [3]. Ultrasonography (US) allows a precise evaluation of the urinary bladder, the proximal abdominal urethra as well as the perineal and penile urethra in male dogs [1]. This modality can detect both radiopaque and radiolucent calculi unless located in the pelvic portion of the urethra. Retrograde urethrography allows the detection of all types of calculi in the entire urethra, but the interpretation can be challenging [3].

In veterinary medicine, urolithiasis can be managed medically or surgically depending on its mineral composition [4]. Retrograde urohydropropulsion and secondary urethral catheterization are performed frequently before cystotomy to restore urethral patency [5]. Despite these procedures, residual calculi remain on the immediate post-operative radiographs following a cystotomy in 14% to 20% of dogs [6-8]. Urethral calculi are detected in more than 50% of dogs with incomplete urolith removal [8]. This may be explained by unsuccessful or incomplete retrograde urohydropropulsion preceding surgery or failure of urethral flushing during surgery.

In human medicine, non-enhanced computed tomography (CT) is the imaging modality of choice for assessing urolithiasis that allows the visualization of all types of calculi, regardless of their chemical composition or size [9]. In a recent study in cats, non-enhanced CT has been used to diagnose ureteral calculi with a superior detection rate to US [10].

In human medicine, *in vivo* CT studies showed good accuracy in predicting the calculus composition using dual-energy CT (DECT) or single-energy non-enhanced CT, with the ability to differentiate uric acid and non-uric acid calculi or uric acid and calcium oxalate calculi, respectively [11-13]. In veterinary medicine, *in vitro* CT studies have been performed with variable results. One demonstrated good accuracy in predicting the canine calculi type using mean beam attenuation measurement in Houndsfield units (mHU) [14]. Another showed that the DECT measurements could not distinguish the common types of canine urolithiasis [15].

The aims of this study were (1) to define the success rate of retrograde urohydropropulsion in male dogs using non-enhanced CT and (2) to determine if the measured mean beam attenuation values could predict the calculus composition. It was hypothesized that non-enhanced CT could detect residual urethral calculi after unsuccessful or incomplete retrograde urohydropropulsion and that *in vivo* mHU measured with CT could help predict the urolithiasis composition. These two topics will be presented separately in this article.

MATERIALS AND METHODS

All dogs and cats presented with lower urinary tract uroliths and having a non-enhanced CT preceding surgery were included from June 2019 to June 2021 at the veterinary hospital (Centre Hospitalier Vétérinaire Pommery, Reims, France). Male dogs that presented with urethral calculi had CT performed after retrograde urohydropropulsion and urinary catheter placement. This study obtained ethical approval from the Comité d'éthique Jacques Bonnod de VetAgro Sup n°18, France (research ethics approval number: 2165).

CT was performed under general anesthesia, without contrast injection, immediately before surgical management. The patients were maintained with isoflurane after induction with diazepam (0.2 mg/kg intravenously), followed immediately by propofol titrated to effect (up to 4 mg/kg intravenously). The patients were positioned in sternal recumbency, and the images of the caudal abdomen were acquired using a single-energy 16-slice CT scanner (Siemens SOMATOM Emotion 16; Siemens Healthcare GmbH, Germany). A 110 kVp and 230 mAs technique was used for cats and dogs under 30 kg, and a 130 kVp and 230 mAs technique was used for dogs over 30 kg. The slice thicknesses and slice increments were respectively 0.75 mm and 0.4 mm for cats and dogs under 15 kg, 1 mm and 0.5 mm for dogs between 15 kg and 30 kg, and 1.5 mm and 0.7 mm for dogs over 30 kg. Reformatted images in the transverse, sagittal, and dorsal planes were obtained and reviewed by a third-year ECVDI resident (A.B.) using three different CT reconstruction algorithms. The algorithms were selected with a "Body" type of kernels for all reconstructions with a "standard" scan mode according to the manufacturer's information. The first algorithm, "B30s," had a low resolution with smooth images and was displayed in a soft tissue window (window width and level of 300 HU and 40 HU, respectively). The second algorithm, "B70s", had a medium resolution with sharp images and was displayed in a bone window (window width and level of 1,500 HU and 450 HU, respectively). The third algorithm, "B90s," had a high resolution with ultrasharp images and was displayed in the same bone window.

For male dogs, the number of cases with persistent calculi in the urethra and their location (prostatic urethra, membranous urethra, perineal urethra, and penile urethra) was recorded.

For each case, the measurement of the calculi attenuation was performed and recorded for each convolution kernel. Each measurement was performed on the transverse images at the level of the maximal diameter of the calculi. A manual region of interest (ROI) was drawn for each calculus assessed to include the largest calculus area without adjacent structures included within the ROI (**Fig. 1**). The mHU and rounded to the first decimal. The average mHU was calculated when two or three calculi were present. When more than three calculi

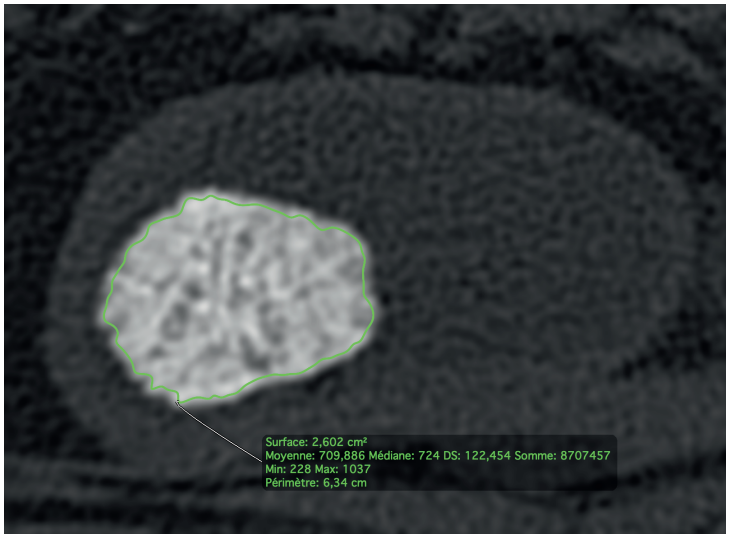

Fig. 1. Manual ROI measurement technique for the mean beam attenuation values. The ROI was drawn as large as possible to include the largest calculus area without adjacent structures. The mHU measured was 710 HU using the convolution filter B90s.
ROI, region of interest; mHUs, mean beam attenuation measurement in Houndsfield units; HU, Houndsfield unit.

https://doi.org/10.4142/jvs.22109

were present, the average of the three largest calculi was calculated. All the measurements were performed without knowledge of the mineral composition.

The records of all uroliths submitted for analysis were reviewed. Quantitative analysis by infrared spectrometry was performed either by a private veterinary laboratory (Vet'analys, France) or the University of Minnesota (Minnesota Urolith Center, United States). Calculi with a predominant component (> 85%) and traces of other components were considered pure mineral composition. Calculi with a mixed composition (predominant component < 85%) were excluded.

Statistical analysis was performed using a statistical software program (R Core Team 2019 software; R Foundation for Statistical Computing, Austria). A graphic evaluation of the data was first assessed. In male dogs, the percentage of cases with persistent calculi in the urethra was calculated. A comparison of the mHU for each convolution filter was conducted using a Kruskal-Wallis Rank Sum Test. The mHU for each convolution filter was compared according to types of calculi using a Pairwise Wilcoxon Rank Sum test. A Wilcoxon test was performed for each type of calculus to compare the mHU obtained in the different convolution filters.

RESULTS

Sixty-five cases were included in the study. There were 55 dogs (45 males and 10 females) and 10 cats (nine males and one female). Forty-one patients were intact, and 24 were neutered. The mean age was 5.9 years old (range: 1–12 years old), and the mean weight was 18.75 kg (range: 1.4–95 kg).

Retrograde urohydropropulsion

Forty-five male dogs underwent retrograde urohydropropulsion for the management of urethral calculi. In these patients, remaining urethral calculi were detected on a CT examination after the procedure in 20 patients (44.4%), indicating a 55.6% success rate of retrograde urohydropropulsion on the first attempt. The remained calculi were located in the membranous urethra in 11 cases (42.3%), in the penile urethra in 10 cases (38.5%), and the prostatic urethra in five cases (19.2%). In six patients, the remaining calculi were detected in two urethral locations: in both the prostatic and membranous urethra in four dogs (**Figs. 2** and **3**) and in both the membranous and penile urethra in two dogs. A repeated retrograde urohydropropulsion

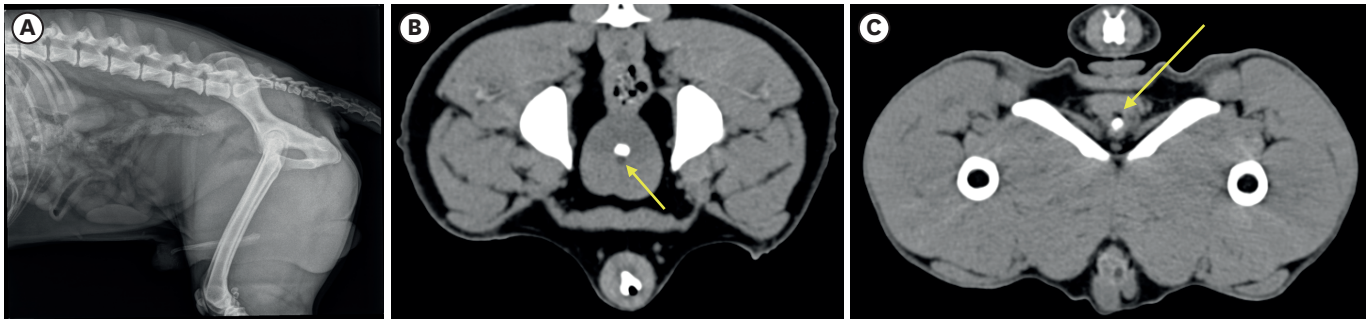

Fig. 2. Radiographic (A) and computed tomographic (B, C) examination of a male Dalmatian dog. No urolithiasis was seen on the right lateral radiographic view of this dog. Two urethral calculi were diagnosed using CT, one in the prostatic urethra (B) and one in the membranous urethra (C). The urinary catheter is visible (yellow arrow) in the urethral lumen next to the calculi showing retrograde urohydropropulsion failure.
CT, computed tomography.

Fig. 3. Computed tomographic examination of a male pug dog with urohydropropulsion failure. Sagittal reformatted computed tomography images (soft tissue algorithm with convolution filter B30s) of the caudal abdomen of a male dog show a prostatic urethral calculus and a membranous urethral calculus with the urinary catheter (yellow arrow) passing next to them.

was attempted in these 20 patients in which the retrograde urohydropropulsion failed, and a second control CT acquisition was performed immediately. Six cases (13.3%) still had persistent calculi, all located within the penile urethra. The success rate of the second retrograde urohydropropulsion was 70%. The global success rate after one or two retrograde urohydropropulsions in dogs was 86.7%, and the global failure rate of the procedure was 13.3%.

Regarding the nine male cats included in the study, the CT examination highlighted four cases with urethral calculi observed adjacent to the urinary catheter. Retrograde urohydropropulsion was attempted afterward and was successful in two cats.

A cystotomy was performed in 64 out of 65 cases (55 dogs and nine cats). Only one male cat did not have a cystotomy. This patient had a single penile urethral calculus still present after the retrograde urohydropropulsion and underwent a perineal urethrostomy.

In male dogs, the urethrostomy was performed in eight cases (six due to persistent urethral calculus and two due to a urethral stenosis without persistent urethral calculus). Urethral stenosis was not visible on CT acquisitions but was demonstrated after a retrograde urethrography. None of the patients had a second surgical procedure within 15 wk following surgery.

Stone composition

Quantitative analysis of urolith by infrared spectrometry of the calculi removed was available for 61 patients that underwent surgery. Sixty analyses were performed by a private veterinary laboratory (Vet'analys) and one by the University of Minnesota (Minnesota Urolith Center). Forty-six calculi had a pure mineral composition, and 14 had a mixed composition with one predominant component. One mixed calculus was composed of equal components, including 50% of calcium oxalate and 50% of carbapatite. It was excluded from the mHU measurement.

Of the 61 patients with quantitative analysis by infrared spectrometry, the CT exams in the three different convolution kernels (**Fig. 4**) were available for 50 cases (37 male dogs,

eight female dogs, and five male cats). The cases were classified according to the primary component of the calculi: 20 were classified as cystine, 15 as struvite, eight as calcium oxalate, and seven as urate. **Table 1** lists the mean and standard deviation of the mHU calculated for the different stone compositions in all reconstruction kernels. Using the convolution filter B30s, there was a significant attenuation difference according to the nature of the calculi (*p* value = 2.945e-06). This difference was particularly significant between the cystine and calcium oxalate (*p* value = 0.00029), cystine and urate (*p* value = 0.00182), calcium oxalate and struvite (*p* value = 0.00059), calcium oxalate and urate (*p* value = 0.00405), and struvite and urate (*p* value = 0.01305). Using the convolution filter B70s, there was a significant difference in attenuation according to the nature of the calculi (*p* value= 4.902e-05). This difference was particularly significant between the cystine and calcium oxalate (*p* value = 0.00029), calcium oxalate and struvite (*p* value = 0.00053), and calcium oxalate et urate (*p* value = 0.00472). Finally, using the convolution filter B90s, there was also a significant difference in attenuation according to the nature of the calculi (*p* value = 5.986e-05). This difference was particularly significant between the cystine and calcium oxalate (*p* value = 0.00028), calcium oxalate and struvite (*p* value = 0.00050), and calcium oxalate et urate (*p* value = 0.00405).

Regarding the struvite calculi, there was no difference between the attenuation value measured in all the convolution filters. On the other hand, there was a significant difference in mHU for the calcium oxalate calculi between the convolution B30s/B70s (*p* value = 0.02201) and B30s/B90s (*p* value = 0.0213). Moreover, there was a significant difference in mHU for the cystine calculi

Fig. 4. Transverse reformatted CT images at the level of the prostatic urethral calculus of a dog. The three different CT reconstruction algorithms are shown: soft tissue algorithm with convolution filter B30s displayed at a window width of 300 and a window level of 40 (A); bone algorithm with convolution filter B70s displayed at a window width of 1,500 and a window level of 450 (B); bone algorithm with convolution filter B90s displayed at a window width of 1,500 and a window level of 450 (C).
CT, computed tomography.

Table 1. Mean and SD of the mHUs calculated for the different stone compositions in all reconstructions

Variables	Number	Kernel	Mean mHUs ± SD
Cystine	20	B30s	723.50 ± 82.24
		B70s	789.00 ± 90.71
		B90s	873.00 ± 172.57
Struvite	15	B30s	708.67 ± 169.03
		B70s	729.33 ± 160.60
		B90s	776.67 ± 159.40
Calcium oxalate	8	B30s	1,643.75 ± 192.73
		B70s	1,831.25 ± 108.79
		B90s	2,012.50 ± 126.86
Urate	7	B30s	498.57 ± 94.33
		B70s	648.57 ± 202.44
		B90s	735.71 ± 294.08

mHUs, mean beam attenuation measurement in Houndsfield units.

https://doi.org/10.4142/jvs.22109

between the convolution B30s/B70s (p value = 0.005367), B30s/B90s (p value = 0.0008354), and B70ss/B90 (p value = 0.002449). Regarding the urate calculi, there was a significant difference in mHU between the convolution B30s/B70s (p value = 0.03552) and B30s/B90s (p value = 0.03603).

Using a threshold of 1,000 HU or greater for the B30s convolution filter (1,100 HU for the B70s convolution filter and 1,500 HU for the B90s convolution filter), a sensitivity and specificity of 100% can be obtained to differentiate calcium oxalate calculi from other types of calculi encountered (**Fig. 5**).

DISCUSSION

Retrograde urohydropropulsion is a routine procedure for managing urethral lithiasis in dogs [5]. In the present study, the global success rate of this procedure, assessed by non-enhanced CT, was 86.7% in dogs. Urohydropropulsion failure could partially explain why 14% to 20% of dogs still have calculi remaining in the lower urinary tract after the cystotomy because 50% of these dogs showed remaining urethral calculi [6-8]. In addition, the presence of urethral calculi in combination with cystoliths increases the risk of cystotomy failure [8]. The present results can be explained by the possibility of persistent calculi in the urethra, located adjacent to the catheter otherwise placed correctly. Non-enhanced CT appears to be an optimal noninvasive technique for imaging uroliths in dogs, allowing an evaluation of the bladder and entire urethra and the visualization of small, radiopaque, and radiolucent calculi after retrograde urohydropropulsion preceding surgery. This technique allows a quick and thorough evaluation of the urethral lumen, owing to its high contrast resolution [10].

Non-enhanced CT has some limitations because it does not detect urethral stenosis. In two cases of the study, urethral stenosis was demonstrated using retrograde urethrography. Therefore, retrograde urethrography is required if urethral stenosis is suspected, particularly in cases of recurrent urethral calculi.

The narrowest parts of the urethra are the penile urethra, as explained by restricted distension due to the penile bone, and the isthmus portion just proximal to the perineal urethra at the level of the ischiatic arch, considered in the present study as a part of the membranous urethra [16]. These anatomical features explain why most of the persistent calculi in this study were observed in the membranous or the penile urethra. The persistence of calculi in the penile urethra was always the cause of retrograde urohydropropulsion failure after the second attempt, requiring urethrostomy. The presence of calculi within the penile urethra should alert the clinician of the possibility of retrograde urohydropropulsion failure.

Epidural anesthesia and general anesthesia can induce muscle relaxation of the urethra during retrograde urohydropropulsion [17]. In this series, mechanical obstruction due to the penile bone in the case of penile urethral calculi may still be a limitation of this procedure.

The second aim of the study was to determine if CT mean beam attenuation measurements can predict the calculus composition and if the choice of the reconstruction kernel can modify the HU measured values. Regarding the mHU measured, despite the significant difference between the mHU for the different types of calculus, overlaps in mHU values were observed, particularly between cystine and struvite calculi, and to a lesser extent, between them and the urate calculi. Hence, an analysis of the calculus is still needed to assess the

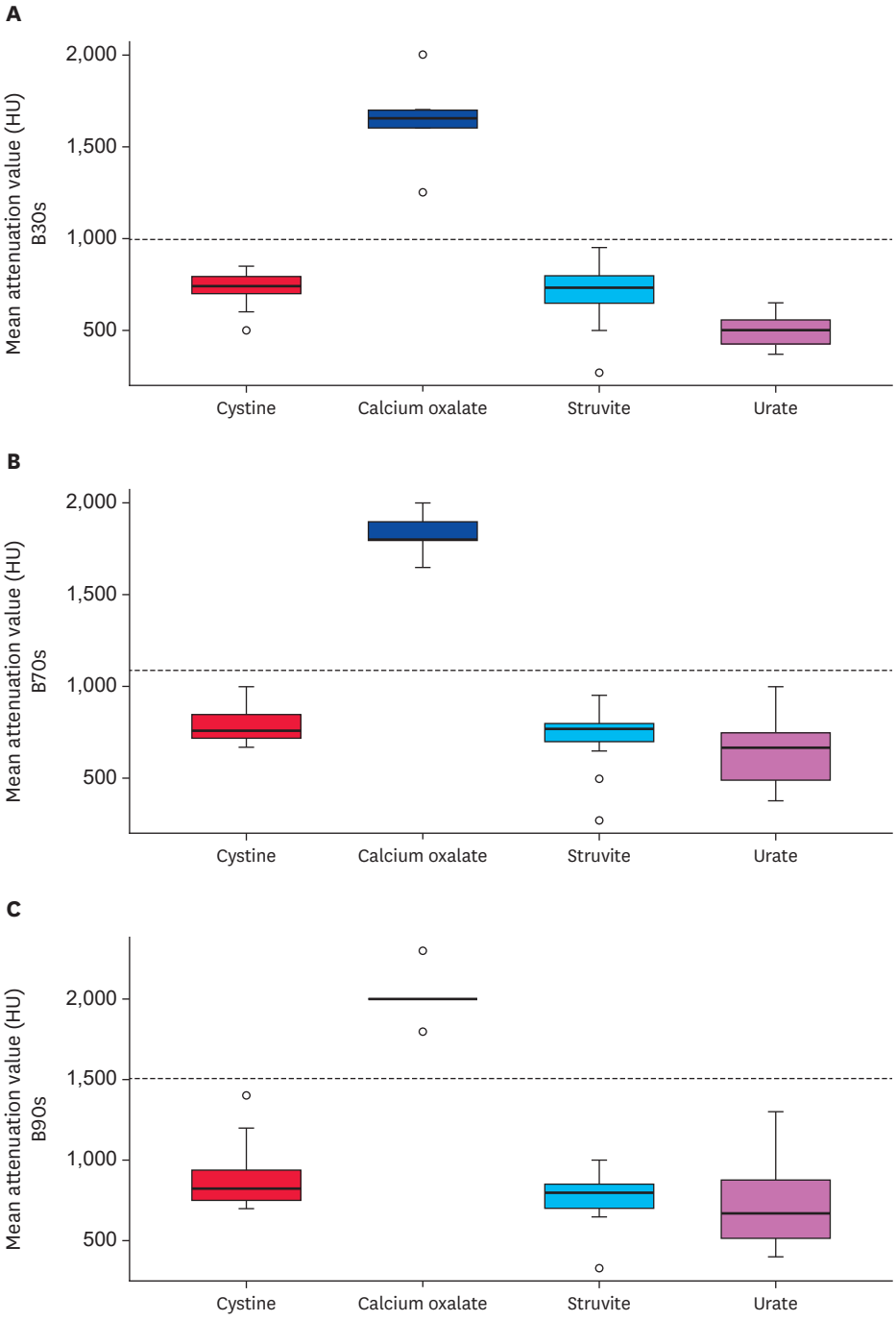

Fig. 5. Boxplots of the CT mHU for the different stone compositions. Using the soft tissue algorithm with convolution filter B30s (A), the bone algorithm with convolution filter B70s (B), and the bone algorithm with convolution filter B90s (C). The short lower and upper lines represent the minimum and maximum. The thick black line represents the median; the central box contains 50% of the values, between the 25% and 75% quartiles. The circles represent the range of values. The dotted line represents the threshold proposed.
CT, computed tomography; mHUs, mean beam attenuation measurement in Houndsfield units; HU, Houndsfield unit.

exact nature. Using non-enhanced CT, calculi with a predominant composition of calcium oxalate can be differentiated from all the other calculus types because they have mHU values that are always superior to 1,000 mHU with the B30s convolution kernel. This proposed threshold is compatible with the mHU measured in a previous *in vitro* study, where all calcium oxalate calculi ranged from 1,363.3 to 1996.5 mHU (using an 80 kVp CT technique)

[14]. Therefore, CT could be used to confirm the need for surgery, lithotripsy, or voiding urohydropropulsion in patients with calculi with an attenuation value > 1,000 HU because medical treatment cannot be attempted in cases of calcium oxalate urolithiasis [4].

A smooth, soft tissue algorithm with convolution filter B30s appears to be the most useful filter. With this kernel, there was a significant difference in all the mHU regarding the calculus composition except between the cystine and struvite calculi. In addition, the convolution kernel influenced the mHU measured values, as demonstrated previously in human medicine [18-20]. Convolution kernels can significantly alter the mHU of tissues from their initial values [18,20] and the sharpness of the kernels affects the values of the quantitative imaging features [19]. According to the literature, the choice of the convolution kernel affects the tissue attenuation measurement; the tube voltage, table height, and field of view also appear to be involved [20]. This may represent another limitation of these results and suggests that the mHU values may potentially vary according to the brand of the CT machine and the settings of the CT examination. Another limitation is that the mHU measurements were performed with hand-drawn ROI in a large range of calculi diameters. Therefore, the accuracy of the mHU measurements for very small calculi could be questioned. For this reason, only the largest three were measured when multiple calculi were present.

The trends in urolith composition described elsewhere [21,22] do not correspond to the results of this study. The proportions of calcium oxalate, struvite, urate, and cystine calculi described previously were 46.2%–47%, 43.6%–47.1%, 9.2%–14.9%, and 2.7%, respectively [21,22]. In contrast, the proportions in the present study were 16%, 30%, 14%, and 40%, respectively. The difference could be explained by the small number of calculi analyzed.

Non-enhanced CT is routinely used to manage uroliths in humans, despite the use of radiation exposure because the received dose is low for a single abdominal acquisition [10]. Non-enhanced CT may avoid failure of clinical management of uroliths in dogs and cats. Hence, the benefits of this rapid, noninvasive and efficient technique may outweigh the deleterious effects of radiation exposure.

In conclusion, this study highlights the utility of non-enhanced CT in managing uroliths in dogs and cats. It can be performed easily and quickly to reduce the risk of incomplete urethral lithiasis removal after retrograde urohydropropulsion. Using non-enhanced CT before surgery could improve the success rate of cystotomy. CT beam attenuation could help predict the urolith types *in vivo*. A mean HU value above 1,000 HU using a soft tissue algorithm with a smooth convolution filter (B30s) is highly predictive of the calcium oxalate calculus and may help determine the treatment plan.

REFERENCES

1. Hotston Moore A. The bladder and urethra. In: O'brien R, Barr F, editors. *BSAVA Manual of Canine and Feline Abdominal Imaging*. 1st ed. Quedgeley: John Wiley & Sons Inc; 2009, 205-221.
2. Marolf AJ. Urinary bladder. In: Thrall DE, editor. *Textbook of Veterinary Diagnostic Radiology*. 7th ed. Missouri: Saunders; 2018, 846-864.
3. Weichselbaum RC, Feeney DA, Jessen CR, Osborne CA, Dreytser V, Holte J. Urocystolith detection: comparison of survey, contrast radiographic and ultrasonographic techniques in an *in vitro* bladder phantom. Vet Radiol Ultrasound. 1999;40(4):386-400.
PUBMED | CROSSREF

4. Lulich JP, Berent AC, Adams LG, Westropp JL, Bartges JW, Osborne CA. ACVIM small animal consensus recommendations on the treatment and prevention of uroliths in dogs and cats. J Vet Intern Med. 2016;30(5):1564-1574.
PUBMED | CROSSREF
5. Osborne CA, Lulich JP, Polzin DJ. Canine retrograde urohydropropulsion. Lessons from 25 years of experience. Vet Clin North Am Small Anim Pract. 1999;29(1):267-281, xiv.
6. Lulich JP, Osborne CA, Polzin D. Incomplete removal of canine and feline urocystoliths by cystotomy. J Vet Intern Med. 1993;7:124.
7. Bevan JM, Lulich JP, Albasan H, Osborne CA. Comparison of laser lithotripsy and cystotomy for the management of dogs with urolithiasis. J Am Vet Med Assoc. 2009;234(10):1286-1294.
PUBMED | CROSSREF
8. Grant DC, Harper TA, Werre SR. Frequency of incomplete urolith removal, complications, and diagnostic imaging following cystotomy for removal of uroliths from the lower urinary tract in dogs: 128 cases (1994-2006). J Am Vet Med Assoc. 2010;236(7):763-766.
PUBMED | CROSSREF
9. Mitcheson HD, Zamenhof RG, Bankoff MS, Prien EL. Determination of the chemical composition of urinary calculi by computerized tomography. J Urol. 1983;130(4):814-819.
PUBMED | CROSSREF
10. Testault I, Gatel L, Vanel M. Comparison of nonenhanced computed tomography and ultrasonography for detection of ureteral calculi in cats: a prospective study. J Vet Intern Med. 2021;35(5):2241-2248.
PUBMED | CROSSREF
11. Basha MA, AlAzzazy MZ, Enaba MM. Diagnostic validity of dual-energy CT in determination of urolithiasis chemical composition: *in vivo* analysis. Egypt J Radiol Nucl Med. 2018;49(2):499-508.
CROSSREF
12. Bonatti M, Lombardo F, Zamboni GA, Pernter P, Pycha A, Mucelli RP, et al. Renal stones composition *in vivo* determination: comparison between 100/Sn140 kV dual-energy CT and 120 kV single-energy CT. Urolithiasis. 2016;8:1-7.
PUBMED
13. Nakada SY, Hoff DG, Attai S, Heisey D, Blankenbaker D, Pozniak M. Determination of stone composition by noncontrast spiral computed tomography in the clinical setting. Urology. 2000;55(6):816-819.
PUBMED | CROSSREF
14. Pressler BM, Mohammadian LA, Li E, Vaden SL, Levine JF, Mathews KG, et al. *In vitro* prediction of canine urolith mineral composition using computed tomographic mean beam attenuation measurements. Vet Radiol Ultrasound. 2004;45(3):189-197.
PUBMED | CROSSREF
15. Nykamp SG. Dual-energy computed tomography of canine uroliths. Am J Vet Res. 2017;78(10):1150-1155.
PUBMED | CROSSREF
16. Byeon YE, Lee ST, Kweon OK, Kim WH. The diameter of maximum distended urethra in male dogs. J Vet Clin. 2009;26(4):331-335.
17. Thiel C, Häußler TC, Kramer M, Tacke S. Urethrolithiasis in the dog - a retrospective evaluation of 83 male dogs. Tierarztl Prax Ausg K Klientiere Heimtiere. 2019;47(6):394-401.
PUBMED
18. Michalski AS, Edwards WB, Boyd SK. The influence of reconstruction kernel on bone mineral and strength estimates using quantitative computed tomography and finite element analysis. J Clin Densitom. 2019;22(2):219-228.
PUBMED | CROSSREF
19. Mackin D, Ger R, Gay S, Dodge C, Zhang L, Yang J, et al. Matching and homogenizing convolution kernels for quantitative studies in computed tomography. Invest Radiol. 2019;54(5):288-295.
PUBMED | CROSSREF
20. Ivanov DV, Kirillova IV, Kossovich LY, Bessonov LV, Petraikin AV, Dol AV, et al. Influence of convolution Kernel and beam-hardening effect on the assessment of trabecular bone mineral density using quantitative computed tomography. Izv Saratov Univ Math Mech Inform. 2020;20(2):205-219.
CROSSREF
21. Kopecny L, Palm CA, Segev G, Westropp JL. Urolithiasis in dogs: Evaluation of trends in urolith composition and risk factors (2006-2018). J Vet Intern Med. 2021;35(3):1406-1415.
PUBMED | CROSSREF
22. Kopecny L, Palm CA, Segev G, Larsen JA, Westropp JL. Urolithiasis in cats: Evaluation of trends in urolith composition and risk factors (2005-2018). J Vet Intern Med. 2021;35(3):1397-1405.
PUBMED | CROSSREF